The hairpin extension controls solvent access to the chromophore binding pocket in a bacterial phytochrome.

1 Supplementary Information

1.1 Introduction to amide exchange-model

The rate of amide exchange in an unstructured random-coil polypeptide is dependent on temperature, pH as well as the primary structure. Using data from model peptides, this intrinsic rate of exchange (k_{int}) can be easily predicted for each amide in a given protein sequence [4]. In a folded protein, the observed rate constants for amide protons are often much slower than the predicted k_{int}. This is due to solvent inaccessibility, protection by H-bonds or both [5]. Exchange occurs in the protected amides by exposure to solvent due to an opening event as outlined in the two-state model in **Eq.** 3.

These opening events can be small fluctuations that expose only a single amide, local unfolding of a larger segment of structure or global unfolding of the protein [6]. Exchange may also occur by small non-cooperative fluctuations that allow water into the protein interior through solvent channels however **Eq.** 3 does not apply in this case [6].

In a typical experiment, the protein is exchanged into deuterium solution and monitored by NMR and/or mass spectrometry [5]. Assuming the two-state model in **Eq.** 3, the observed rate constant for exchange, k_{obs}, is dependent on the microscopic rate constants k_{op}, k_{cl} respectively and k_{int}. Under native conditions, $k_{cl} \gg k_{op}$ and the observed rate constant for exchange, k_{obs}, is given by [5]:

$$k_{obs} = \frac{k_{op}k_{int}}{k_{cl} + k_{int}} \tag{S1}$$

Two limits exist for exchange depending on the relative magnitudes of the rate constants. At the EX2 limit, $k_{cl} \gg k_{int}$ and k_{obs} simplifies to:

$$k_{obs} = \frac{k_{op}}{k_{cl}}k_{int} \tag{S2}$$

At the EX1 limit, $k_{int} \gg k_{cl}$ and therefore k_{op} becomes rate limiting and k_{obs} simplifies to:

$$k_{obs} = k_{op} \tag{S3}$$

When k_{cl} and k_{op} are of similar magnitude, the kinetics usually have two phases with rate constants [7]:

$$k_{1,2} = \frac{B \pm \sqrt{B^2 - 4A}}{2} \tag{S4}$$

where $A = k_{op}k_{int}$ and $B = k_{op} + k_{cl} + k_{int}$ and amplitudes [7]:

$$A_1 = \frac{k_2 - k_{int}f_o}{k_2 - k_1}, A_2 = \frac{k_{int}f_o - k_1}{k_2 - k_1}, A_1 + A_2 = 1 \tag{S5}$$

where f_o is the fraction of molecules in the open state at time zero which can be written in terms of K_{eq}: $f_o = K_{eq}/(1 + K_{eq})$ where $K_{eq} = k_{op}/k_{cl}$.

1.2 SI Materials and Methods

For pH titration measurements, the stock solutions of the phytochromes in the dark state were diluted into solutions buffered between pH 6 and 11: Mes buffer was used for pH 6 to 7.1, Tris for pH 7.2 to 9.2 and glycine for pH 9.3 to 11. The final concentration of buffer was 30 mM with constant ionic strength maintained at all pH values using NaCl. The final concentrations of the protein constructs were ~2 μM giving an absorbance at 700 nm of about 0.25 at pH 8. incubating in the dark for approximately 3 hours, the absorbance spectrum of each sample was measured in the dark using a Cary 8454 UV-vis spectrometer (Agilent Technologies).

The pH jump in the illuminated Pfr state was performed as described in the main text except, before the dilution, the sample was illuminated with a red LED light (655 nm with output power of 7 mW corresponding a photon flux of about 490 μmol m^{-2} s^{-1}) for 2 min. For CBD-PHY, the dark reversion is very slow with about 2 % conversion to Pr in 50 min [8] and so had minimal effect on the observed kinetics.

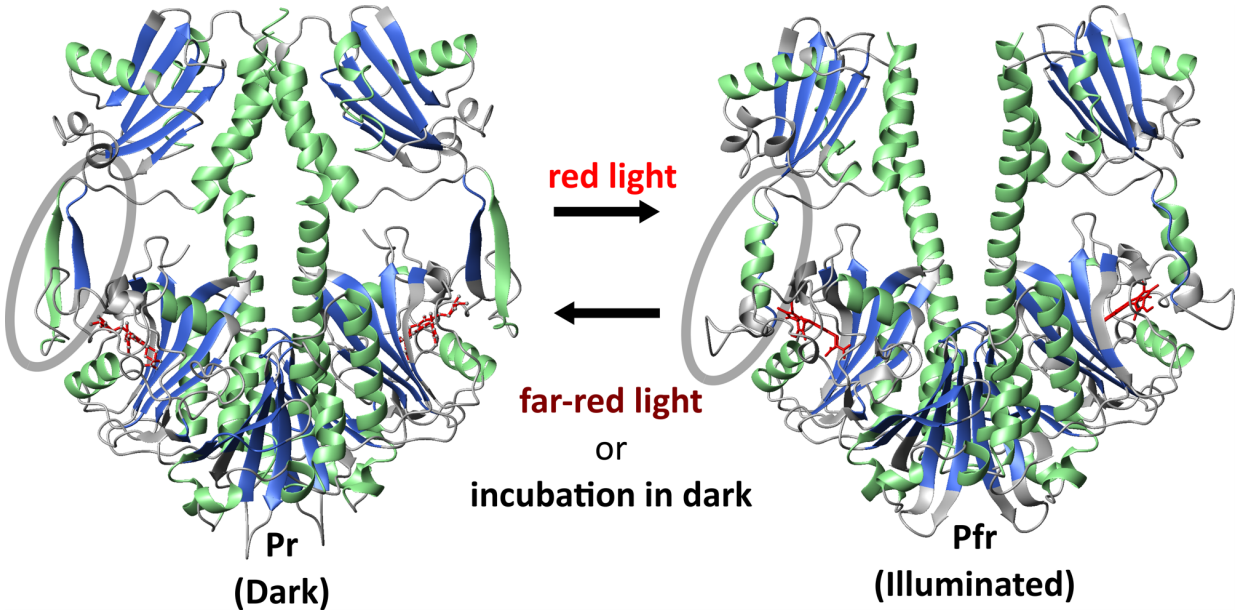

Fig. S1 Structure of CBD-PHY in the Pr and Pfr state The crystal structure of CBD-PHY in the Pr and Pfr state are shown colour coded according to the secondary structure predicted using Jpred 4 [1] (predicted α-helix is green, predicted β-strand is blue, the remaining is grey). The BV chromophore is shown as sticks coloured red. The predicted structure type generally matches with the structure type observed in crystals except for the hairpin extension circled in grey. Figure made using PDB files 4O0P [2] and 5C5K [3].

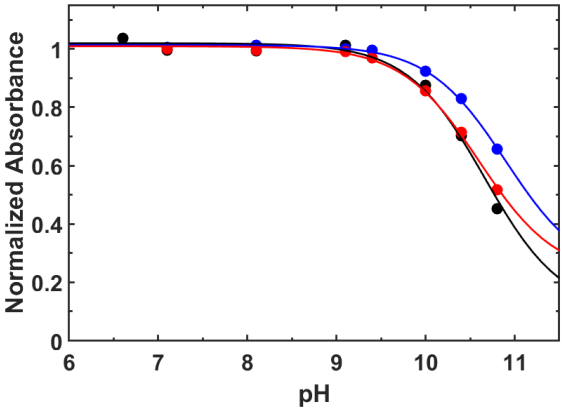

Fig. S2 Absorbance-monitored pH titration The absorbance at 700 nm as a function of pH is plotted for CBD-PHY WT[9] (blue), CBD-PHY Y263F[9] (red), and CBD (black). Experimental details can be found in Supplementary Materials and Methods. Lines represent a fit to a single pK_a model with pK_a values of 10.9, 10.6 and 10.7 for CBD-PHY WT, CBD-PHY Y263F and CBD respectively. Note that the model is under-determined by the data and any fitted parameters are therefore an approximation (See more details in [9])

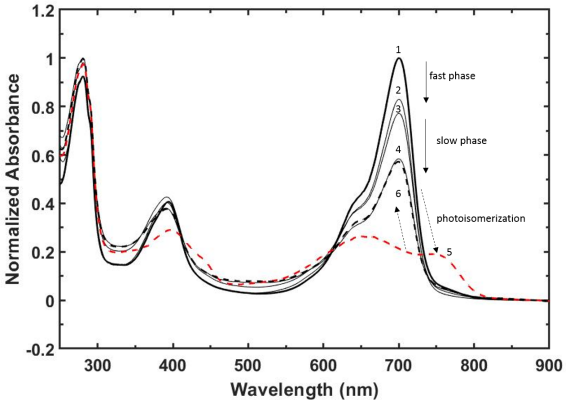

Fig. S3 Absorbance monitored pH jump of CBD-PHY in the dark Pr state and reversible photoisomerization after long incubation at pH 10.8 Spectra are normalized to the absorbance at 700 nm of CBD-PHY in the Pr state in pH 8.0 buffer (scan 1, thick solid line). Absorbance scans are taken after 13 seconds (scan 2) 12 minutes (scan 3) and 150 minutes (scan 4) after dilution into pH 10.8 (thin solid lines). Red light illumination of the sample with prolonged pH 10.8 incubation results in a typical "Pfr" peak at 750 nm (scan 5, short dashed red line, see also **Fig.** S4) which can be reversed to the same Pr spectrum upon illumination with far red light (scan 6, short dashed black line).

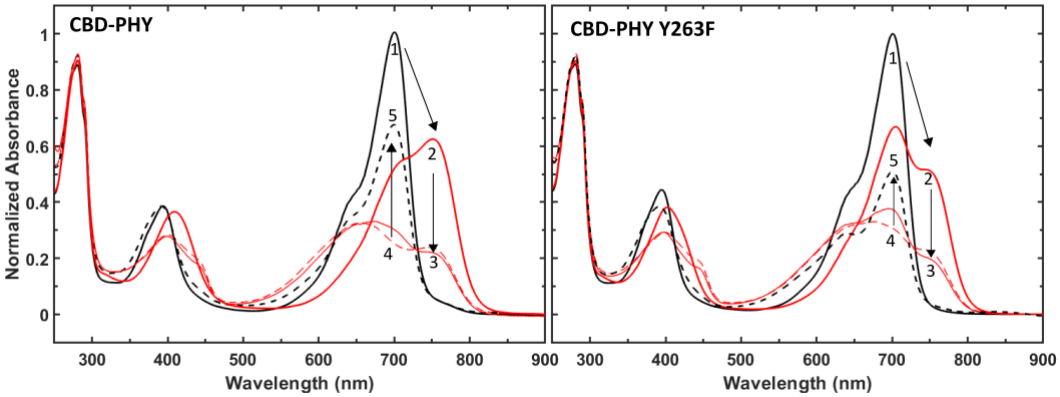

Fig. S4 Determination of endpoint absorbance for pH jump kinetics and fast deprotonation observed in the Pfr state Spectra are normalized to the absorbance at 700 nm in the Pr state in pH 8.0 buffer (scan 1, solid black line). The Pfr state at pH 8.0 is formed after illumination with red light indicated by the increased absorbance at 750 nm (scan 2, solid red line). Approximately 30 % of the population remains in the Pr state due to overlapping Pr and Pfr spectra. A decrease in absorbance is observed 13 seconds after a pH jump from 8.0 to 10.8 (scan 3, thin red line). Measurement at later time points shows a small decrease in absorbance in the 700 nm "Pr peak" but not in the 750 nm "Pfr peak". This indicates deprotonation is fast in the Pfr state and that BV is not protected from solvent exchange. Further illumination with red light slightly increases the 750 nm absorbance indicating the population can be driven further to the Pfr state at high pH (scan 4, red dashed line). Note that the resulting spectra is the same if the phytochrome in the Pr is first diluted into pH 10.8 and then illuminated with red light. Formation of the Pr state at pH 10.8 is observed after illumination with far red light (scan 5, dashed black line). This is the absorption spectrum that is expected for the phytochrome protein at equilibrium protonation at pH 10.8.

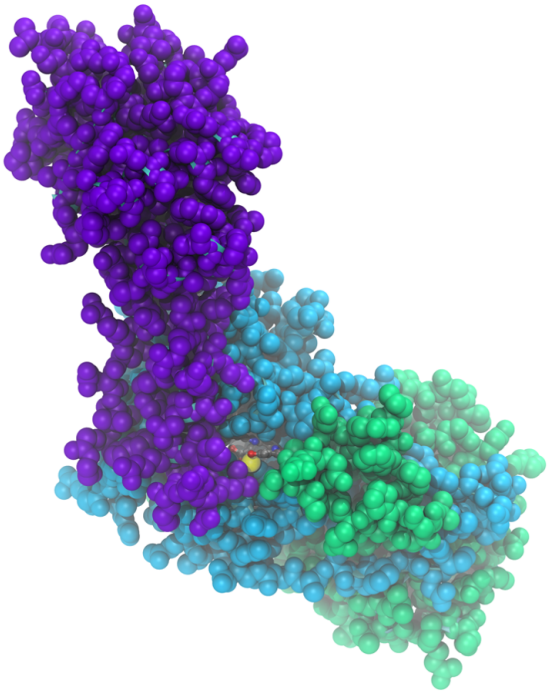

Fig. S5 Solvent exposure of the CBD-PHY binding site in the Pfr state Crystal structure of CBD-PHY in the illuminated Pfr state coloured according to domains as in **Fig.** 1.

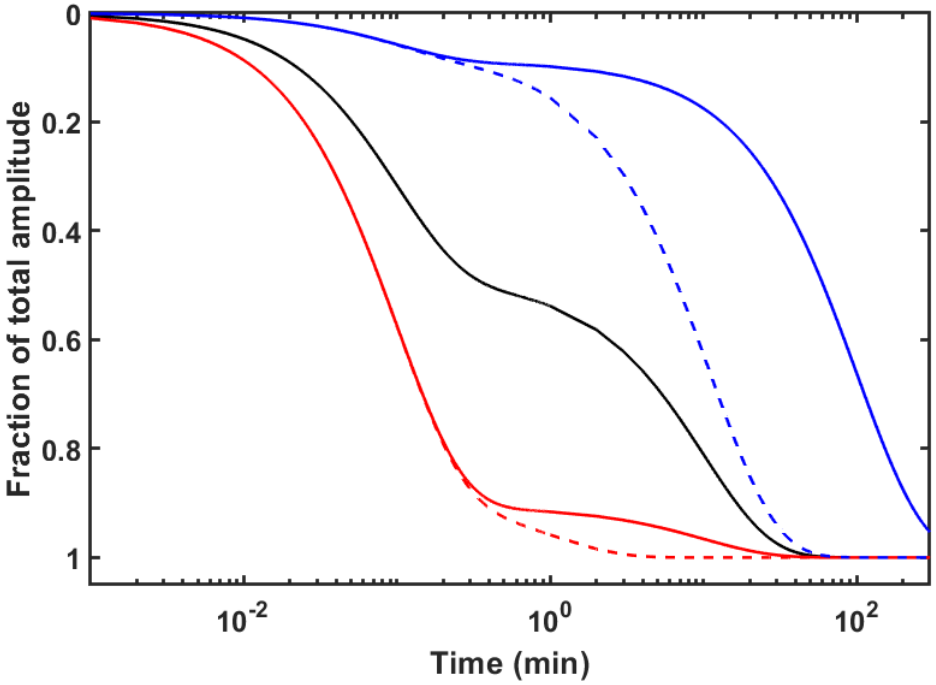

Fig. S6 Effect of k_{op} and k_{cl} on the observed kinetics and relative amplitudes of BV deprotonation Data was simulated using **Eqs.** S4 and S5. The k_{op} was 10 min^{-1} for all simulations. The other rate constants with units of min^{-1} were as follows:

— Blue solid $k_{op} = 0.01$ and $k_{cl} = 0.1$, $K_{eq} = 0.1$ and $fAmp_1$ is 0.1
--- Blue dashed $k_{op} = 0.1$ and $k_{cl} = 1$, $K_{eq} = 0.1$ and $fAmp_1$ is 0.1
— Black solid $k_{op} = 0.1$ and $k_{cl} = 0.1$, $K_{eq} = 1$ and $fAmp_1$ is 0.5
— Red solid $k_{op} = 0.1$ and $k_{cl} = 0.01$, $K_{eq} = 10$ and $fAmp_1$ is 0.9
--- Red dashed $k_{op} = 1$ and $k_{cl} = 0.1$, $K_{eq} = 10$ and $fAmp_1$ is 0.9

References

1. A. Drozdetskiy, C. Cole, J. Procter, B. G.J., Nucleic Acids Res **43**(W1), W389 (2015)
2. H. Takala, A. Björling, O. Berntsson, H. Lehtivuori, S. Niebling, M. Hoernke, I. Kosheleva, R. Henning, A. Menzel, J.A. Ihalainen, S. Westenhoff, Nature **509**(7499), 245 (2014)
3. E.S. Burgie, J. Zhang, R.D. Vierstra, Structure **24**(3), 448 (2016)
4. B. Y, J. Milne, L. Mayne, Englander, Proteins. **17**(1), 75 (1993)
5. D. Wildes, S. Marqusee, in *Energetics of Biological Macromolecules, Part E*, *Methods in Enzymology*, vol. 380 (Academic Press, 2004), pp. 328–349
6. J. Clarke, L.S. Itzhaki, Current Opinion in Structural Biology **8**(1), 112 (1998)
7. H. Qian, S.I. Chan, Journal of Molecular Biology **286**(2), 607 (1999)
8. H. Takala, H. Lehtivuori, H. Hammarén, V.P. Hytönen, J.A. Ihalainen, Biochemistry **53**(45), 7076 (2014)
9. J.A. Rumfeldt, H. Takala, A. Liukkonen, J.A. Ihalainen, Photochem. Photobiol. **95**(4), 969 (2019)